Experimental observation of angular correlation between Rydberg electrons in the Ba $n'l'nl$ autoionizing series

R. R. Jones and T. F. Gallagher
Department of Physics, University of Virginia, Charlottesville, Virginia 22901
(Received 1 February 1990)

We have observed the Ba $n'p_{1/2}np$ and $n'p_{1/2}nd$ double Rydberg series ($n > 60, n' < 0.75n$) using a five-laser excitation scheme. A single photon excites the $n'p_{1/2}nl$ levels from an initially populated Ba $8s_{1/2}nl$ autoionizing state. If there were no correlation between the two valence electrons, we would observe only the $n'pnp$ or $n'pnd$ states. However, we observe strong excitation to $n'snl$ and $n'dnl$ states as well. We observe virtually no $n'snl$ and $n'dnl$ states for $n' < 0.4n$. For $n' > 0.75n$ the Rydberg structure that is observed for the lower n' levels disappears into an apparently unstructured continuum.

I. INTRODUCTION

While the problem of an atom with two correlated electrons has been studied since the early days of quantum mechanics, recent interest in the problem dates from the experiments of Madden and Codling,[1] who observed the correlated doubly excited states of He converging to the $n = 2$ states of He^+. Since their work on He, there has been a significant amount of both experimental and theoretical work. Most of the former has been carried out using either synchrotron radiation or electron scattering, both of which suffer from relatively poor resolution. In contrast, laser excitation holds out the promise of high resolution, and over the past few years tunable laser experiments have approached the double-ionization limit of alkaline-earth atoms. While laser excitation offers high resolution, it is hampered by the fact that the energies required to reach even the lowest double-ionization limits, those of the alkaline-earth atoms, are greater than 15 eV, far in excess of the photon energies available using current tunable laser technology. A common approach in studying the alkaline-earth atoms is to populate a bound Rydberg state just below the first ionization limit and use two-photon excitation or multistep excitation through real intermediate states to reach the vicinity of the double-ionization limit.[2-5]

Recently Camus *et al.*[2] have observed evidence of electronic correlation in two-photon transitions from bound Ba $6snp$ and $6snd$ states to doubly excited states near the second ionization limit. Starting from the $6snp$ states, one expects to observe only the $n'snp$ and $n'dnp$ states by a two-photon excitation of the inner electron with the outer electron remaining a spectator. However, when starting from the $6s45p$ state, for example, only for $n' < 25$ are only $n'snp$ and $n'dnp$ states observed. For $25 < n' < 32$ the $n'pnl$ and $n'fnl$ series are observed as well, and for $n' > 32$ the spectrum degenerates into an apparently unstructured continuum. The observation of the $n'pnl$ and $n'fnl$ states is attributed to Stark mixing of the inner electron wave function by the electric field from the outer electron. This mixing is the onset of correlation between the two electrons.

Here we report analogous, but more extensive, observations in an experiment in which we would expect to observe only the Ba $n'pnd$ states. Our experiments differ from those of Camus *et al.*[2] in several ways. We have used higher values of the principal quantum numbers of both electrons, different angular momentum series ($n'pnd$ and $n'pnp$), and most important, a sequential excitation through intermediate autoionizing states. Our experiments, and similar ones by Eichmann, Lange, and Sandner[5] that focused on the Ba $n'gnd$ states, demonstrate clearly the generality of the observations of Camus *et al.*[2] In the following sections we describe our experimental approach, present our results, and consider what conclusions may be drawn from the collected results.

II. EXPERIMENTAL PROCEDURE

Our excitation scheme involves the use of four or five pulsed tunable dye lasers as shown in Fig. 1. When $n'pnd$ levels are produced, two dye lasers are used to place the ground-state atoms in a $6snd$ level. The first dye laser drives the Ba $6s^2$-$6s6p\ ^1P_1$ transition and the second laser then excites a $6snd$ Rydberg state. A third tunable dye laser then excites a $6p_{3/2}nl$ autoionizing state. The frequency of this third laser is set at the Ba^+ $6s$-$6p_{3/2}$ transition and the Ba $6snl$-$6pnl$ transition is, in essence, an ion transition with the Rydberg electron remaining as a spectator.[6] The frequency of the fourth dye laser is fixed at one half of the Ba^+ $6p_{3/2}$-$8s_{1/2}$ interval. When this fourth dye laser is frequency doubled it may excite either a Ba^+ ion in a $6p_{3/2}$ state to an $8s_{1/2}$ state or a neutral Ba $6p_{3/2}nd$ autoionizing state to an $8s_{1/2}nd$ autoionizing state. A fifth dye laser is then used to excite the Ba $n'pnl$ double Rydberg state, and we detect the Ba^+ Rydberg-state product of autoionization.

When $n'pnp$ levels are excited the ground-state atoms are driven to a $6snp$ Rydberg level by a single photon. This Rydberg atom then undergoes the same three final excitations discussed above. Thus, for this case, only four dye lasers are necessary.

A diagram of the apparatus is shown in Fig. 2. For case d (i.e., for excitation of $n'pnd$ levels) the first two dye

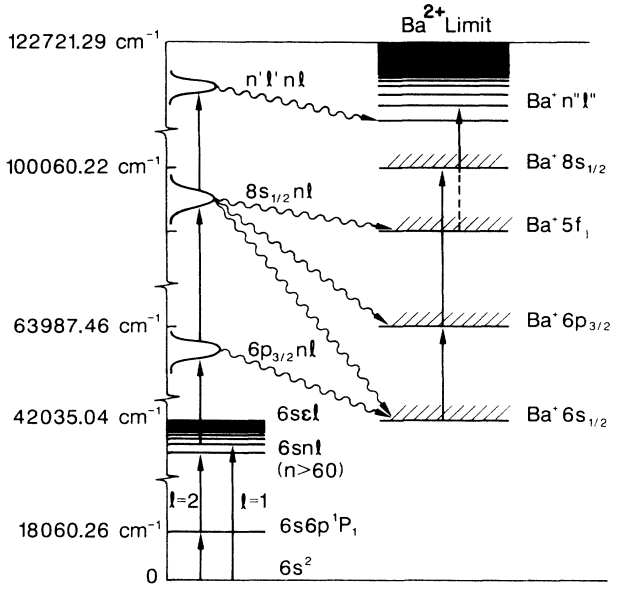

FIG. 1. Diagram of the laser excitation scheme showing important intermediate levels, but not drawn to scale. One or two pulsed dye lasers excite Ba atoms to a high-n ($n > 60$) $6snp$ state using a single photon or to a $6snd$ state via a $6s6p$ intermediate state. The $6snl$ Rydberg atoms are then excited to a $6p_{3/2}nl$ autoionizing state. Another dye laser excites this autoionizing state to an $8snl$ level. A final laser drives the $8snl$-$n'l'nl$ transition. Note that the lasers also excite ion levels after the autoionization of intermediate states.

lasers are pumped by an excimer laser operating with XeCl at 308 nm. The first laser is frequency tuned to the Ba $6s^2$–$6s6p\ ^1P_1$ resonance at 18 060.26 cm^{-1}.[7] This laser is of the Hansch[8] type and has a linewidth of $\simeq 0.8$ cm^{-1}. The second commercial dye laser is tuned to excite a $6snd$ Rydberg level. It has a frequency of $\simeq 24\,000$ cm^{-1} and a linewidth of 0.05 cm^{-1}. Both of these dye lasers have pulse energies of $\simeq 100$ μJ and pulse widths of 10 ns. For case p (i.e., for excitation of $n'pnp$ levels) the commercial laser light is frequency doubled in a beta barium borate (BBO) crystal to produce ultraviolet light at $\simeq 240$ nm that is used to excite a $6snp$ Rydberg level. Hereafter we will refer to the initial excitation to a Rydberg state as a single step. The lasers that drive the final three transitions will be referred to as the second, third, and fourth lasers for both p and d excitations to avoid confusion.

The last three dye lasers are of the Hansch[8] type, are pumped by different harmonics of an Nd:YAG (yttriuum aluminum garnet) laser, and have pulse widths of 10 ns. The second dye laser is pumped by the Nd:YAG third harmonic and has its frequency fixed at the Ba^+ $6s_{1/2}$-$6p_{3/2}$ transition at 21 952.42 cm^{-1}.[7] This laser has a linewidth of 1 cm^{-1} and a pulse energy of $\simeq 100$ μJ. The third dye laser has its frequency fixed at 18 036.38 cm^{-1} and is amplified before being frequency doubled by a potassium dihydrogen phosphate (KDP) crystal. The doubled light has a frequency which matches the Ba^+ $6p_{3/2}$-$8s_{1/2}$ transition at 36 072.76 cm^{-1},[7] a linewidth of $\simeq 2$ cm^{-1}, and a pulse energy of $\simeq 50$ μJ. The fourth dye laser is also amplified and can be tuned from near 23 000 to 24 000 cm^{-1} to excite different final states of the core electron. This laser has a pulse energy of $\simeq 1$ mJ and a linewidth of 0.7 cm^{-1}. All of the dye lasers are operated at a 20-Hz repetition rate.

The dye laser beams interact with an effusive Ba beam originating from a resistively heated oven in a vacuum chamber with a background pressure of 10^{-7} Torr. The lasers enter the vacuum chamber parallel to each other and at a right angle to the atomic beam. A 50-cm focal length quartz lens focuses the lasers to a spot of diameter $\simeq 0.5$ mm centered between a pair of 8×8 cm^2 aluminum plates which are separated by 1.0 cm. After the lasers are fired a voltage pulse is applied to the lower aluminum plate that field ionizes the Ba^+ Rydberg states which are the products of decay of the neutral $n'pnl$ levels. This pulse accelerates both singly and doubly ionized Ba through a 0.6-cm-diam hole in the center of the upper plate. Note that the rapid rise time (< 0.5 μs) of the field pulse allows the Rydberg ions to sample large electric fields (> 10 kV) before leaving the field region. The hole in the upper plate is covered by a fine stainless-steel mesh

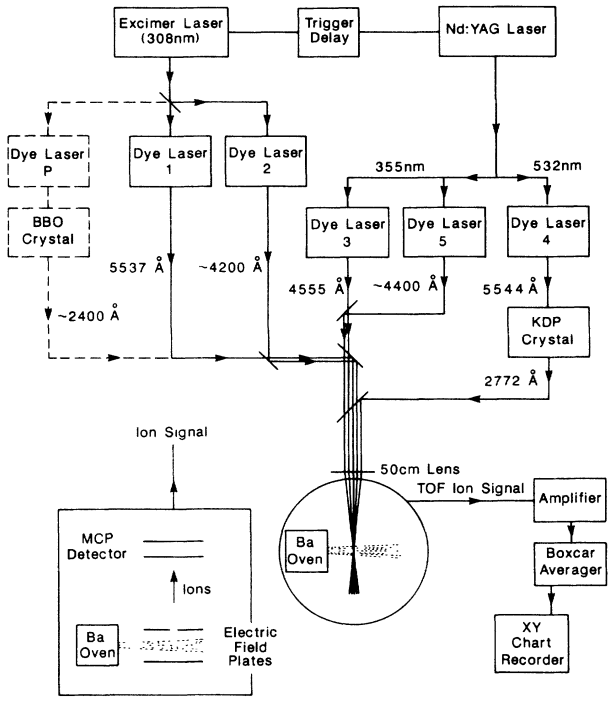

FIG. 2. Schematic of the basic experimental apparatus showing the laser and detection equipment. The laser apparatus consists of an Nd:YAG and a XeCl excimer pump laser and five tunable dye lasers. The fundamental output of dye laser 4 is frequency doubled in a potassium dihydrogen phosphate (KDP) crystal. The lasers interact with an effusive Ba beam between a pair of parallel aluminum plates. We field ionize the Ba^+ Rydberg states which are the products of autoionization and detect the singly and doubly charged ions with a microchannel plate (MCP) detector in our time-of-flight (TOF) spectrometer. When $6snp$ states are excited, lasers 1 and 2 are replaced with laser p and the BBO frequency-doubling crystal.

which helps to preserve the electric field homogeneity in the interaction region. After leaving the interaction region, the ions travel through a distance of $\simeq 10$ cm before striking a dual microchannel plate detector. The ion current is then amplified and sent to a boxcar averager. For these measurements we study the Ba^{2+} signal, which is clearly time resolved from the Ba^+ signal by the different flight times of the two ions.

For excitation of these double Rydberg levels, the temporal positions of the final three dye lasers (lasers 2, 3, and 4) are extremely critical. The first laser(s) precedes the other three by approximately 100 ns. This temporal separation ensures that only Ba atoms in the ground state or in a $6snl$ Rydberg level are in the interaction region when the other lasers appear. Laser 3 and laser 4 appear in the interaction region $\simeq 2$ ns before laser 2. By delaying laser 2 by approximately one-half of its temporal width, we ensure that atoms which are excited to a $6p_{3/2}nl$ autoionizing state will see the maximum field of lasers 3 and 4 at the instant that they are excited. This temporal positioning enhances the population in the final states by ensuring that the excitation rate out of the $6p_{3/2}nl$ state is at a maximum when these intermediate levels are populated.

In both excitation schemes the field ionization pulse appears approximately 200 ns after the appearance of the last laser. This delay time ensures that there is no electric field in the interaction region during the laser pulses. Dispersion of the small excited volume due to the space charge of the Ba ions after the final excitation decreases the resolution of the time-of-flight (TOF) ion signal. The slow degradation of resolution with increasing delay times between the lasers and field ionization pulse sets an upper limit on the delay time used. For core states with principal quantum number $n' < 30$ our electric field pulse does not have sufficient amplitude to ionize the autoionization decay products. Therefore for these states we use the Nd:YAG laser fundamental (1064 nm) to photoionize the Ba^+ Rydberg levels.

III. EXPERIMENTAL RESULTS

We have experimentally observed the frequency dependence for excitation of $n'l'nl$ autoionizing states from $8s_{1/2}n''l''$ levels for $l''=1$ or 2, $n''=60$–75, and $n' > 30$. For values of $n'' < 60$ the population of the intermediate autoionizing states is depleted at a rate much greater than the rate of final-state population. Thus, for these levels no significant double Rydberg excitation is observed. However, since the lasers driving the second and third transitions have frequencies which match the ion transitions we do observe direct excitation of Ba^+ ion Rydberg series. Our spectra show excitation of the Ba^+ $np_{1/2}$, nd, and ng ion series. The $np_{1/2}$ series is excited by the final laser excitation from Ba^+ $8s_{1/2}$ levels and the nd and ng levels are reached from Ba^+ $5f$ levels which are reached through autoionization of the $8s_{1/2}nl$ levels. These ion transitions are observed for the entire range of states we have studied, and they serve as markers for accurate frequency calibration.[9,10]

Due to the n^{-3} scaling of the autoionization rates of the $6pnl$ and $8snl$ levels the amount of population which can be placed in the final double Rydberg states is greatly increased by slight increases in the principal quantum number of the "outer" nl electron. This effect is shown in Figs. 3 and 4 where we show frequency scans of the final laser for different states of the "outer" electron. Figure 3 shows excitation of states which are nominally $n'pnd$ and Fig. 4 shows $n'pnp$ levels. Note the obvious increase in the signal-to-noise ratio as the principal quantum number of the "outer" electron is increased. The ion transitions mentioned previously are labeled on the scans and are the dominant features for lower values of n. For higher values of n the ion excitation and neutral excitations become comparable as decay of the intermediate states becomes slower. Also, the fact that Figs. 3 and 4 show nearly identical structure indicates that the excita-

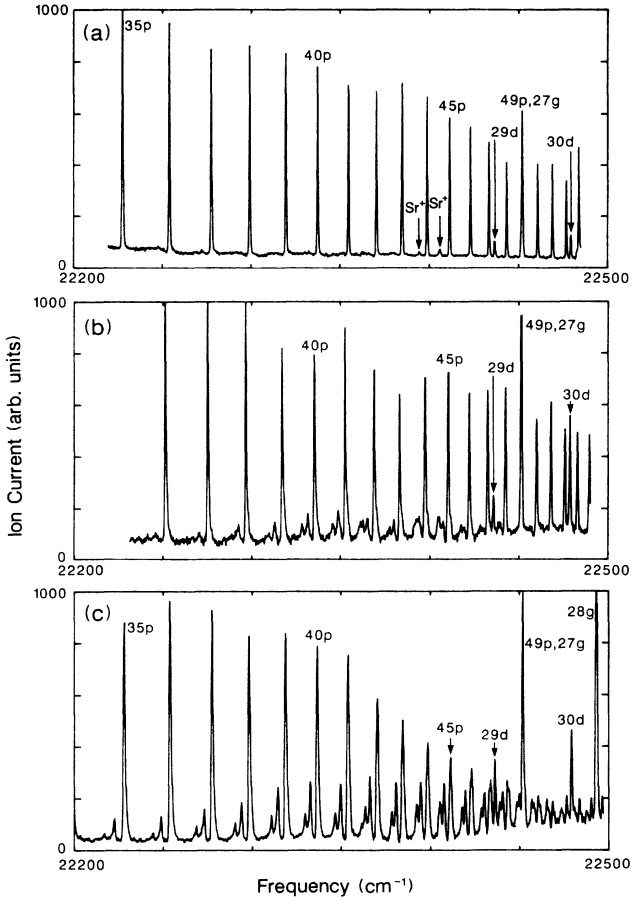

FIG. 3. Frequency scans of the final dye laser over the nominal $n'pnd$ series for (a) $n=54$, (b) $n=66$, and (c) $n=72$. Note the labeled Ba^+ $n'p$, $n'd$, and $n'g$ ion series which are also excited. The obvious increase in the ratio of the amplitude of the neutral series to the ion series is due to the increased lifetime of the intermediate $6p_{3/2}nd$ and $8s_{1/2}nd$ autoionizing states. The Ba^+ $n'p$ series is nearly degenerate with the $n'pnd$ series for the lower values of n' but for larger values of n' the feature broadens and shifts, indicating that the neutral level is present. Also, note that the neutral Ba features are smoothed into an unstructured continuum for $n' > 0.75n$.

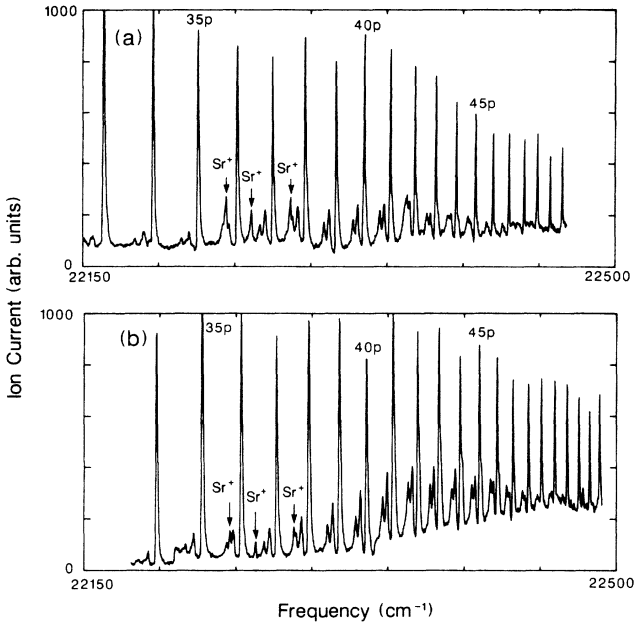

FIG. 4. Frequency scans of the final dye laser over the nominal $n'pnp$ series completely analogous to Fig. 3 with (a) $n=64$ and (b) $n=70$. Comparison of this figure with Fig. 3 clearly shows that the angular momentum of the "outer" electron has only minimal effect on the appearance of the final spectrum.

tion of the final $n'l'nl$ levels is not very sensitive to the angular momentum of the "outer" electron. It is also interesting to note that the application of a small electric field, which mixes the l states of the outer electron, also produces an increase in the signal-to-noise ratio, without noticeably altering the observed spectra.

As discussed in Sec. II, the effects of the space charge of the electrons and ions which are produced from autoionization can be clearly seen by examining the temporal appearance of the ion signal. However, the fact that we are able to see clean excitation of $Ba^+ np$ Rydberg states for $n \simeq 80$ suggests that there are no substantial electric fields in the interaction region when the laser pulses are present. The number of Ba^+ ions produced by the lasers is independent of the principle quantum number of the "outer" electron. Thus the absence of any Stark structure in Fig. 3(a) can be used as direct evidence that there are no substantial microfields in the interaction region during the laser excitation, and that the additional structure seen in Figs. 3(b), 3(c), and 4 are not due to any external fields. Clearly, the space-charge effects only become important over time scales which are significantly larger than the 5-ns laser pulse widths.

Figures 3 and 4 show three dominant features due to excitation of neutral double Rydberg levels. These features are labeled as s, p, and d cores for reasons which will be discussed shortly. Unfortunately, the p core levels are partially or totally obscured by the ion resonances. This fact makes relative cross-section measurements between the different core states virtually impossible.

We obtain the labeling of the core states through plots similar to the one shown in Fig. 5. By measuring the energy imparted to the core electron at each feature in the frequency scans of the final laser we obtain the effective quantum numbers of the core electron for the observed resonances. All of the resonances are assigned a quantum defect and these quantum defects (modulo 1) are plotted versus the integer part of their effective quantum number $+1$. Also shown in Fig. 5 are the quantum defects of the Ba^+ ion s, p, d, and f series.[7,9,10] The levels corresponding to the data near the left-hand side of the plot can be

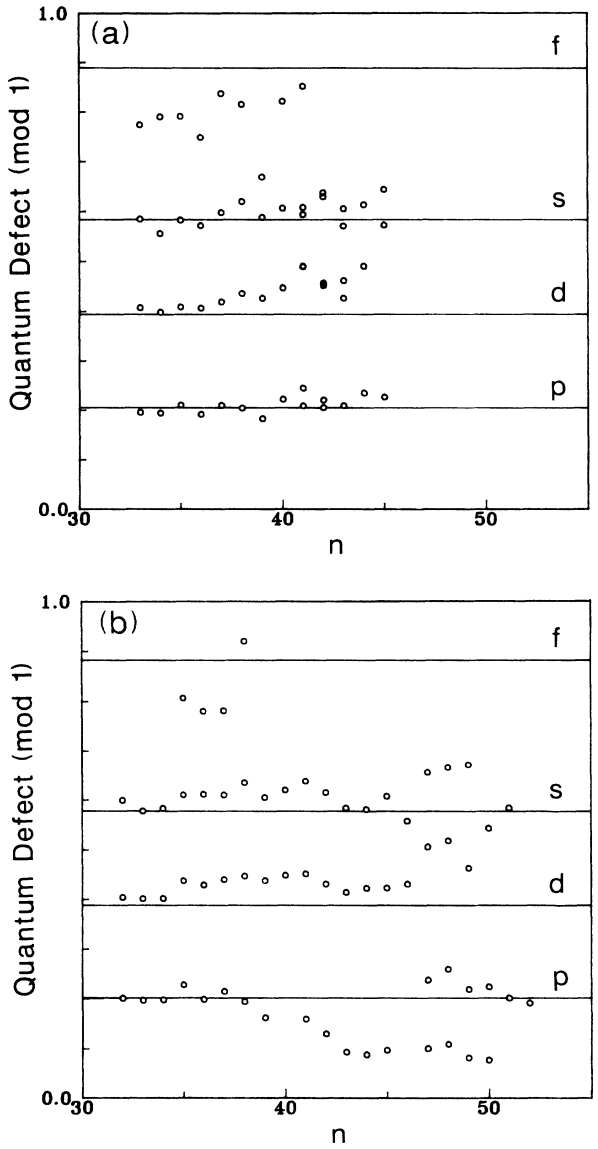

FIG. 5. Plot of the observed quantum defects (mod 1) vs effective quantum number for the observed resonances in the excitation of nominal (a) $n'p66d$ and (b) $n'p73d$ states. The solid lines drawn with the data represent the quantum defects of the s, p, d, and f ion series. In (b) the repulsion of the $n'pnl$ series by the $n'dnl$ and $n'snl$ series is clearly evident. For the larger values of n' the $n'pnd$ and Ba^+ $n'p$ series are clearly resolved and the quantum defects of both are shown to demonstrate the accuracy of the frequency calibration.

clearly labeled as s, p, d, or f core states. Near the right-hand side of the plot the observed resonances clearly do not have a single core configuration. Indeed, an obvious electric dipole interaction can be observed as the p channel repels the s and d channels. The fact that we observe several different core angular momentum levels with minimal energy shifts suggests that angular correlations between the two electrons appear prior to any radial correlation. As the principal quantum number of the core electron approaches that of the outer electron, radial correlations appear and cause energy shifts in the level positions of the different core channels.

Unfortunately, we are unable to assign widths to the observed features on the basis of these data. Although the observed $n'l'nl$ states have widths greater than the laser linewidth the full width at half maximum of these profiles is approximately constant for all values of n'. We believe that the experimental widths are predominantly due to saturation broadening[11] of the final states. However, due to the relatively small size of the $n'l'nl$ signal, attenuation of the fourth laser to a level where saturation broadening is negligible yields insufficient ion current for an accurate linewidth determination.

IV. DISCUSSION

We can summarize the observations from several experiments on Ba $n'l'nl$ states as follows. For $n' < 0.4n$ only the expected series of $n'l'nl$ states is observed. For $0.4 < n' < 0.7n$, $n'l' \pm 1nl$ series are observed as well. As n' approaches $0.7n$ the sharp $n'l'nl$ features decrease in intensity and are obscured by an apparent continuum which increases in intensity. In the region $0.4n < n' < 0.7n$ there is a very obvious repulsion of the spectral features originating from the $n'l'nl$ and $n'l' \pm 1nl$ series.

The above observations are all consistent with a Stark-effect description of the correlation between the two electrons. Specifically, the outer electron is assumed to produce a static field over the inner electron's orbit, which leads to both anomalous features in the observed spectra, the presence of the $n'l' \pm 1nl$ states, and the repulsion of the $n'l'nl$ and $n'l' \pm 1nl$ states. In all the experiments to date there has not been sufficient resolution to allow quantitative statements about the l distribution of the outer electron, and this point has been generally ignored. It has, however, implicitly been taken into account. As pointed out by Eichmann, Lauge, and Sandner,[5] if the outer electron is assumed to be fixed at its most probable radius (near its outer turning point), its field at the inner electron's orbit is precisely that required to produce the observed spectra. Assuming that the outer electron remains at its classical turning point is approximately equivalent to assuming that it is in one of the extreme Stark states, or in a state of high angular momentum. The former are mixtures of l states and are therefore accessible from lower-lying states in which the outer electron is in a well-defined l state. A state in which the outer electron has a high angular momentum is of course inaccessible by our excitation scheme. This line of reasoning suggests that the states which have been observed are those with the outer electron in a state somewhat like an extreme Stark state. The states with the outer electron in a Stark state other than an extreme one are in principle accessible, but may yield spectral features too broad to be easily observed. In sum, one may construe the experimental evidence as indicating that the good two-electron states may be roughly approximated by products of Stark states of the two electrons. This picture is similar to one class of theoretical models of doubly excited states for states in which both electrons have the same principal quantum number.[12]

Of course the correct two-electron wave function cannot be a simple product of two single-electron Stark wave functions. The single-electron Stark states, often used to describe the atomic structure in an external electric field, are such that the total angular momentum of the atom is not conserved. In the case of the double Rydberg states discussed here, total angular momentum J is conserved. Thus, a better representation of the localized two-electron states may be a linear superposition of products of two angular momentum eigenstates, with each product in the sum conserving angular momentum separately. The correct wave function is then a sum of product wave functions not a product of single-electron Stark wave functions.

The success of the Stark model in reproducing the double Rydberg spectra may be attributed in part to the fact that the resolution of the experiments to date has been too poor to resolve different angular momentum states of the "outer" electron. Therefore, the apparent structure is the same as would be expected from a two-particle wave function consisting of a product of a Stark wave for the inner electron and a single angular momentum wave for the outer electron. Indeed, we observe virtually no difference in the spectra observed with the outer electron in an $l = 1$ or 2 eigenstate or a field-induced Stark state.

In sum it appears that the Stark-effect picture of Camus *et al.*[2] applies quite generally, and may be a partial confirmation of one class of theoretical model. To improve our understanding will require that we better identify the states of the outer electron.

ACKNOWLEDGMENTS

This work has been supported by the National Science Foundation. We would like to acknowledge stimulating discussions with W. Sandner.

[1]R. P. Madden and K. Codling, Phys. Rev. Lett. **10**, 516 (1963).

[2]P. Camus, T. F. Gallagher, J.-M. Lecomte, P. Pillet, L. Pruvost, and J. Boulmer, Phys. Rev. Lett. **62**, 2365 (1989).

[3]N. Morita, T. Suzuki, and K. Sato, Phys. Rev. A **38**, 551 (1988).

[4]R. R. Jones and T. F. Gallagher, in *Abstracts of the 16th International Conference on the Physics of Electronic and Atomic Collisions, New York, 1989,* AIP Conf. Proc. No. 205, edited

by A. Dalgarno, R. S. Freund, M. S. Lubell, and T. B. Lacatorto (AIP, New York, 1990).
[5]U. Eichmann, V. Lange, and W. Sandner, Phys. Rev. Lett. **64**, 274 (1990).
[6]W. E. Cooke, T. F. Gallagher, S. A. Edelstein, and R. M. Hill, Phys. Rev. Lett. **40**, 178 (1976).
[7]C. E. Moore, *Atomic Energy Levels,* Natl. Bur. Stand. (U.S.) Circ. No. 467 (U.S. GPO, Washington, D.C., 1949), Vol. 3.
[8]T. W. Hansch, Appl. Opt. **11**, 895 (1972).
[9]J. Boulmer, P. Camus, J.-M. Gagne, and P. Pillet, J. Phys. B **20**, L143 (1987).
[10]R. R. Jones and T. F. Gallagher, J. Opt. Soc. Am. B **6**, 1467 (1989).
[11]W. E. Cooke, S. A. Bhatti, and C. L. Cromer, Opt. Lett. **7**, 69 (1982).
[12]D. R. Herrick, Adv. Chem. Phys. **52**, 1 (1983).